ELSEVIER

Materials Science and Engineering A 485 (2008) 643–650

MATERIALS SCIENCE & ENGINEERING A

www.elsevier.com/locate/msea

Influence of processing temperature on the microstructures and tensile properties of 304L stainless steel by ECAP

C.X. Huang [a,*], G. Yang [b], Y.L. Gao [b], S.D. Wu [a], Z.F. Zhang [a,*]

[a] *Shenyang National Laboratory for Materials Science, Institute of Metal Research, Chinese Academy of Sciences, Shenyang 110016, China*
[b] *Central Iron and Steel Research Institute, Beijing 100081, China*

Received 11 May 2007; received in revised form 13 August 2007; accepted 23 August 2007

Abstract

304L austenitic stainless steel was successfully processed by equal channel angular pressing (ECAP) in the temperature range of 500–900 °C, and the influences of processing temperature on the microstructures and tensile properties were investigated. At temperature below 700 °C, the microstructures were characterized by lamellar structures and many bundles of deformation twins, which led to a high tensile strength but low elongation-to-failure. With increasing the processing temperature up to 800 °C, dynamic and also static recovery took place and more equiaxed subgrains with low dislocation density were obtained. Deformation twins were found to form only in some grains in the form of individual bands. A low strength and a high elongation-to-failure were achieved compared with those processed at low temperature. The best combination of both high strength and large elongation took place at the processing temperature of 800 °C.
© 2007 Elsevier B.V. All rights reserved.

Keywords: Stainless steel; ECAP; Microstructure; Deformation twins; Tensile strength; Elongation

1. Introduction

Austenitic stainless steels (SSs) are widely used engineering materials mainly due to their excellent corrosion and oxidation resistance. However, their low yield strength is often a major drawback. To strengthen the stainless steel, microstructure/grain refinement is an effective approach [1,2]. It is now well established that processing through the application of severe plastic deformation (SPD), typically, equal channel angular pressing (ECAP), is especially effective in grain refinement for those bulk polycrystalline metals [3]. Up-to-date, this method has been successfully used to produce several ultrafine-grained (UFG) steels, such as low-carbon steels [4,5], ferrite–martensite dual-phase steels [6], etc. As a result, the UFG steels exhibited superior mechanical properties, such as high strength and sometimes good ductility, compared with their coarse-grained (CG) counterparts [5–8].

During the process of ECAP, many processing parameters can affect the deformation structures of materials. They are the die angle, which determines the strain introduced into the material during each deformation pass [9]; the pass number, which corresponds to the total accumulated strain applied to the material; the processing route, which involves rotating the billet between passes [10,11]; the processing speed [12] and the processing temperature [13]. Among these parameters, the effect of processing temperature has been investigated in several materials, such as Al [14], Al–Mg alloys [13,15] and Cu [16]. Increasing the processing temperature (up to 300 °C) caused a fast dynamic recovery in Al and Al–Mg alloys, which resulted in an increase of grain size and the grain shape becoming more equiaxed-like [13–15]. Compared with Al deformed by ECAP at similar homologous temperature (~$0.32T_m$, 150 °C), the distinct difference in the deformation microstructure of Cu was the presence of dynamic recrystallization [16]. It is well known that dynamic recovery/recrystallization occurs easily in those materials with medium-high stacking fault energy (SFE) after large plastic strain. Reduction of SFE decreases the rate of dynamic recovery and facilitates the occurrence of deformation twinning. Recently, 316L SS was processed by ECAP and both dynamic recovery/recrystallization and deformation twinning were observed at temperature as high as 800 °C (~$0.6T_m$) [17]. The occurrence of deformation twinning implies that twinning might be beneficial to the microstructure/grain refinement

* Corresponding authors. Tel.: +86 24 8397 8029; fax: +86 24 2389 1320.
E-mail addresses: chxhuang@imr.ac.cn (C.X. Huang), zhfzhang@imr.ac.cn (Z.F. Zhang).

0921-5093/$ – see front matter © 2007 Elsevier B.V. All rights reserved.
doi:10.1016/j.msea.2007.08.067

of austenitic SS at high processing temperature. Accordingly, the mechanical properties of 316L SS displayed different features, such as apparent tension–compression asymmetry at lower processing temperature and an increase of toughness at higher processing temperature [17].

By checking the materials processed by ECAP in literature, most of them are relatively soft, such as Cu [16], Al alloys [13–15], Fe [18] and low-carbon steel [4,5]. These materials can be processed at RT in order to obtain a good grain refinement effect. However, for hard material, such as SS [17,19], Ti alloys [19,20], Ni–Ti shape memory alloy [21] and W [22], they were commonly processed at elevated temperature due to the limitation of processing conditions. Therefore, the processing temperature becomes an important parameter that can affect the microstructure and related mechanical properties of these materials obviously. As to SS, though there have been several studies on the microstructure/grain refinement of SS processed by SPD [23–27], the application of ECAP to SS is still quite rare and the influences of the processing temperature on the deformation microstructures and corresponding mechanical properties are not adequately explored. In this work, 304L austenitic SS was selected to be processed by ECAP for one pass in the temperature range from 500 to 900 °C. The main goal is to investigate the influences of processing temperature on the microstructures and room-temperature (RT) tensile properties developed by ECAP.

2. Experimental procedure

A hot-rolled commercial AISI 304L type austenitic SS was used in this investigation. The chemical composition of the material is in weight percent of 0.025 C, 18.75 Cr, 10.96 Ni, 0.005 S, 0.0068 P, 0.36 Si, <0.5 Mn, and the balance Fe. The hot-rolled billet was annealed at 1150 °C for 2 h. Samples for ECAP processing were cut from the as-annealed billet with dimension of Ø8 mm × 45 mm.

The ECAP experiments were conducted using a split die with two channels intersecting at inner angle of 90° and outer angle of 30°, which yields an effective strain of ∼1 by a single pass. Before extrusion, the die was preheated to 300 °C and the samples were heated up to the deformation temperature and held for 10 min. Samples were pressed for only one pass at a pressing speed of ∼9 mm/s and at high temperatures of 500, 600, 700, 800, and 900 °C, respectively. After pressing, the samples were cooled in air to RT.

The microstructures on the transverse cross-sections of the as-pressed samples were observed by both optical microscope (OM) and JEM-2000FXII transmission electron microscope (TEM, operating at 200 kV). For OM, samples were ground on SiC paper, polished and etched in a solution of 10% Cr_2O_3 + 90% ethanol. While for TEM, thin foils were first mechanically ground to about 40 μm thick and then finally thinned by a twin-jet polishing facility using a solution of 10% perchloric acid and ethanol at room temperature.

Tensile specimens with a dog-bone shape were cut from the as-pressed billets with the tensile axes oriented parallel to the extrusion direction. The gauge dimension of the tensile specimens is 1.5 mm × 3.0 mm × 15 mm. Tensile experiments were performed on an Instron 8871 testing machine at a constant crosshead speed of 1 mm/min at room temperature.

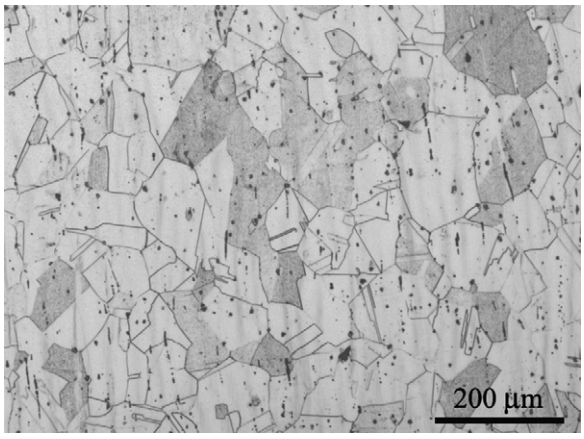

Fig. 1. Optical microstructure of the initial state.

3. Results and discussion

3.1. Microstructure observations

3.1.1. Optical microstructures

Fig. 1 is the optical microstructure of the stainless steel after hot-rolling and annealing at 1150 °C for 2 h. The microstructures are characterized by equiaxed grains with grain sizes in a range of 40–120 μm. Additionally, there are some annealing twins with orientations varying from grain to grain. Inclusions with sizes of several micrometers can only be detected occasionally.

Figs. 2(a)–(f) present the typical optical microstructures of the samples after ECAP processing at different temperatures. It can be seen that for the samples processed at low temperature, below 800 °C (Fig. 2(a)–(d)), the deformation microstructures mainly consist of severely elongated grains, as well as very high density of lamella in the interior of some grains. One of the detailed deformation structures for the sample processed at 500 °C is enlarged and shown in Fig. 2(b). As indicated by the white arrows, many parallel thin lamellae with alternative dark-bright contrast were formed and curved together along certain crystallographic habit plane. Similar deformation structures were also observed in other austenitic steels during tension and are believed to be deformation twins [28]. With increasing the processing temperature, the microstructures display the following characteristics (see Fig. 2(e) and (f)): (a) the shape of grains became equiaxed-like; (b) the density of lamella in grain interior decreased significantly. Fig. 2(g) is a high magnification image of the sample processed at 900 °C, showing that the grains are almost lamella-free. These deformation features suggest that deformation twinning is not prevalent any more at such high temperature.

3.1.2. TEM microstructures

TEM observations were carried out in order to characterize the deformation microstructures in detail. In most cases, two kinds of deformation microstructures were observed, i.e. defor-

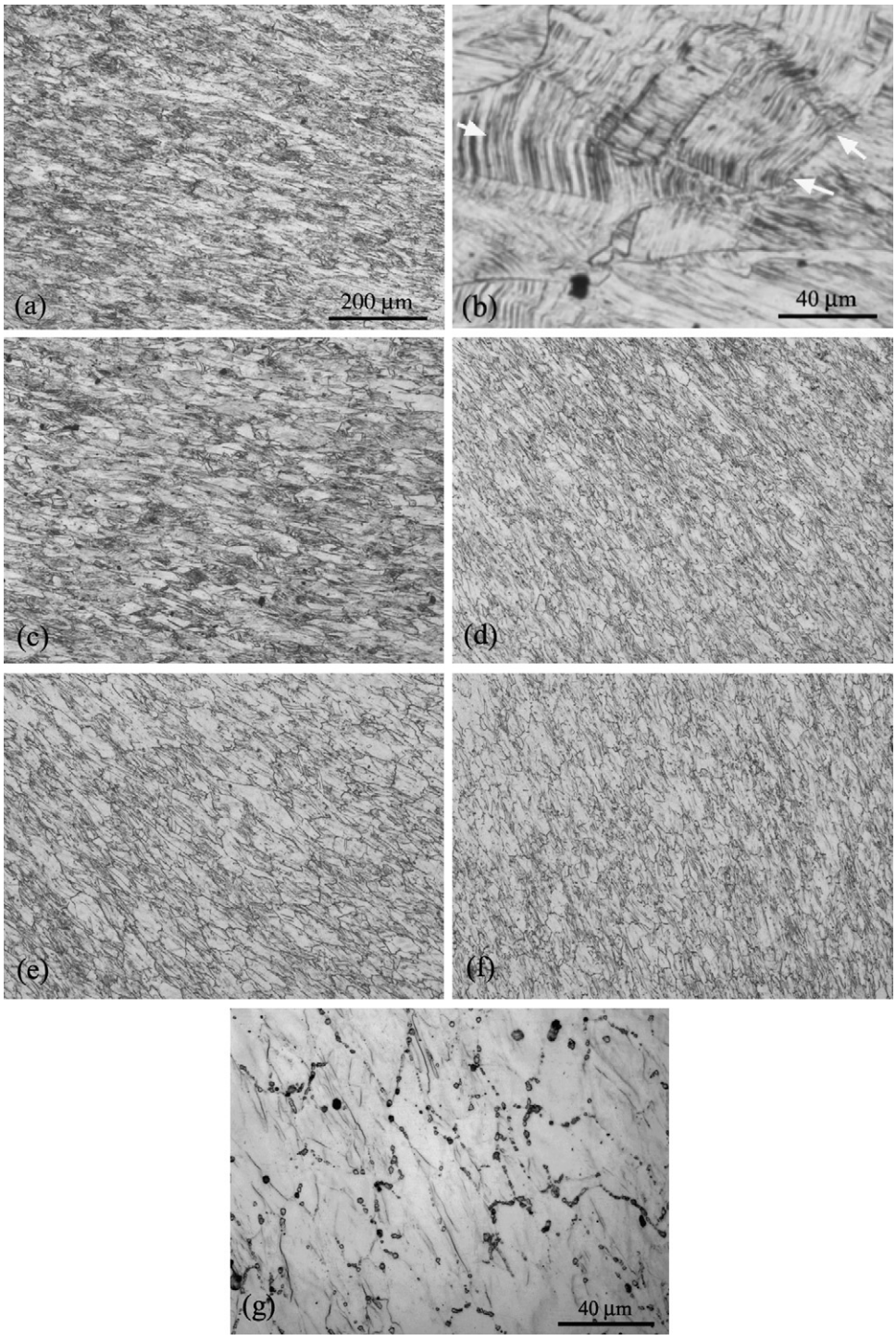

Fig. 2. Optical microstructures of the samples processed at: (a and b) 500 °C, (c) 600 °C, (d) 700 °C, (e) 800 °C and (f and g) 900 °C, respectively. The staff gauges of (c–f) are as same as that of (a). The arrows in (b) indicate twin lamellae.

mation bands/subgrains and deformation twins. Fig. 3(a)–(e) present the typical bright-field TEM micrographs of the samples processed at different temperatures, showing the microstructures of deformation bands and subgrains. The sample processed at 500 °C is mainly composed of band structure with a band width of 100–500 nm, as shown in Fig. 3(a). With increasing temperature, the band structure becomes weak gradually and well-developed subgrains are formed. After processed at 600 and 700 °C, the elongated subgrains are formed usually in deformation bands, as seen in Fig. 3(b) and (c). Further increasing temperature up to 800 and 900 °C leads to more equiaxed-like subgrains (Fig. 3(d) and (e)). The typical size of subgrains in all the samples is of 200–1000 nm. The higher the processing temperature is, the coarser the subgrains are. The formation of subgrains can be confirmed by the corresponding selected-area diffraction (SAD) patterns in Fig. 3(a)–(e), respectively.

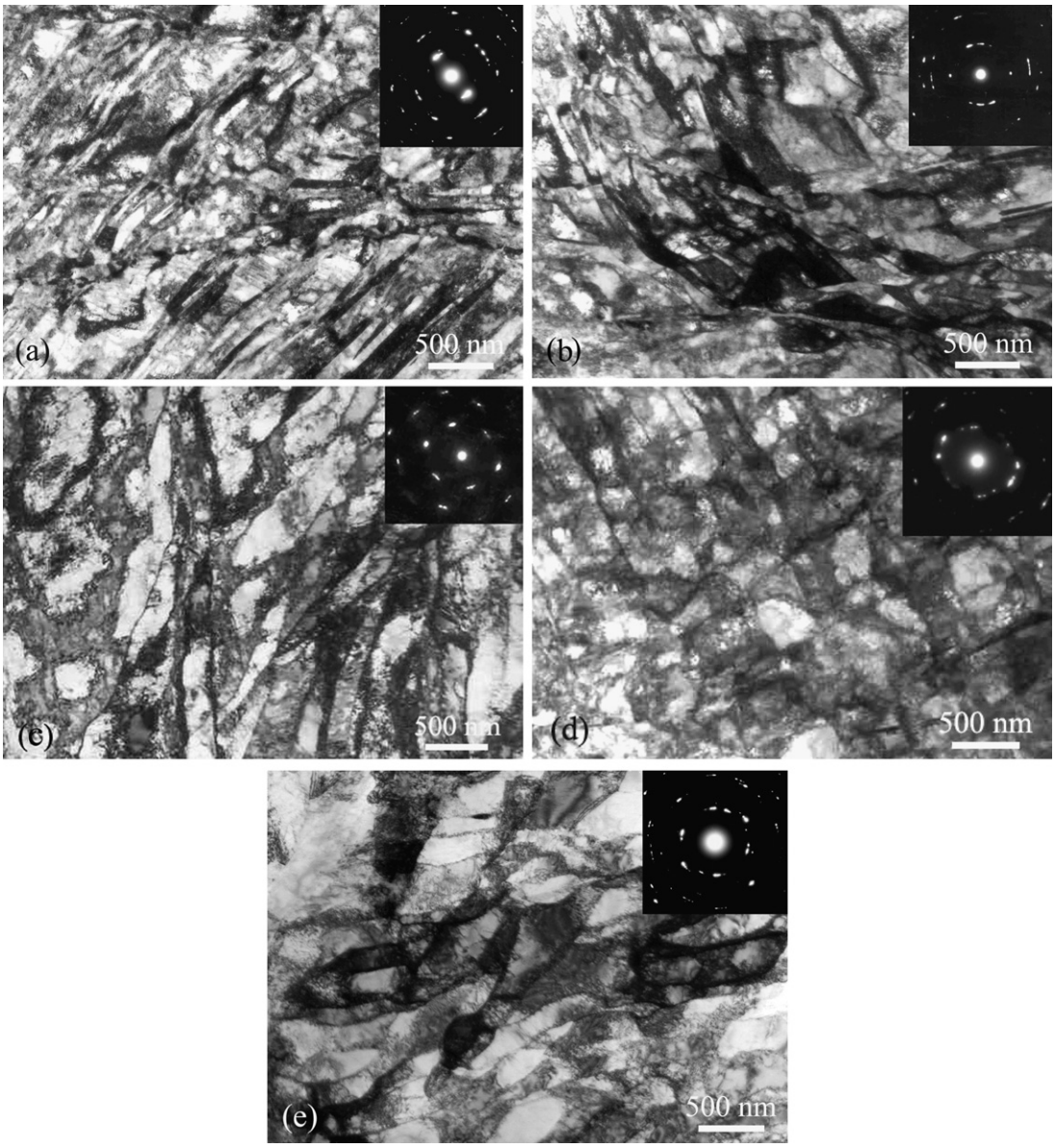

Fig. 3. Bright-field TEM micrographs with corresponding SAD patterns showing the microstructures of the samples processed at: (a) 500 °C, (b) 600 °C, (c) 700 °C, (d) 800 °C, and (e) 900 °C.

It is seen that the spots in the SAD patterns are elongated and formed discontinuous rings, which indicates that low angle grain boundaries have developed during processing.

It should be noted that the grain refinement and formation of equiaxed subgrains at high temperature might be associated with dynamic and also static recovery during pressing and cooling. As shown in Fig. 4(a) of the sample processed at 800 °C, hot deformation leads to the formation of dislocation substructures, such as cells and dense dislocation walls (DDWs) subdividing the original grain into fine blocks. It has been shown in recent works on severe warm and hot deformation of Cu, Al alloy and 304L SS [23,24,29,30], that DDWs evolved eventually into high-angle grain boundary (HAGB, see Fig. 4(a)) via dislocation rearrangement, which was mostly assisted by dynamic recovery. This phenomenon of strain-induced continuous reaction assisted by dynamic recovery was sometimes called as continuous dynamic recrystallization [23,29,30]. As a result, new equiaxed fine grains with low dislocation density were obtained. In the present case, the subgrains produced at high pressing temperatures are characterized by a little larger size, relatively lower dislocation density and more equiaxed shape (Figs. 3(c)–(e) and 4(a)) in comparison with those of the samples processed at low temperature. Besides, HAGB is also created, as shown in Fig. 4(a). All of the phenomena mentioned above imply that dynamic and sometimes static recoveries have taken place during hot pressing. Additionally, recrystallization grains with sizes no more than 1 μm were also observed somewhere in the sample processed at 900 °C, as shown in Fig. 4(b).

In addition to deformation bands and subgrains, deformation twins were also observed, especially in the samples processed at temperature below 700 °C. Fig. 5(a) and (c) are the typical TEM micrographs taken from the samples processed at

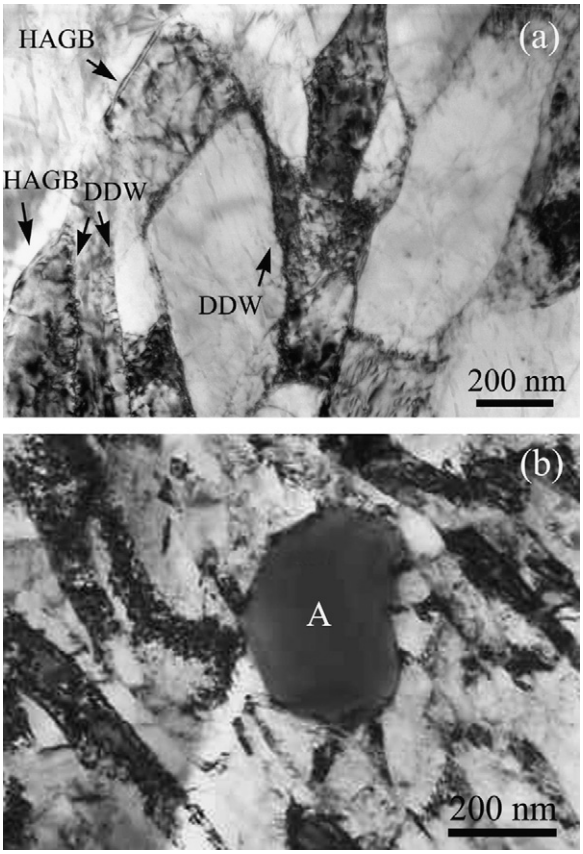

Fig. 4. (a) TEM micrograph of strain-induced subboundaries developed during pressing at 800 °C. The sharp contrast and appearance of boundary fringes in the upper-left part suggest that the boundary is a high angle grain boundary (HAGB). (b) Recrystallized grain, marked with 'A', observed in the sample processed at 900 °C. Note the size of the grain is much larger than that of the neighboring cells/subgrains.

500 and 600 °C, respectively. As indicated by arrows, deformation twins with very thin thickness of 20–50 nm are widely observed and most of them appear in the form of bundles. The twin bundles are not very straight but curving somewhere. Fig. 5(b) is the corresponding SAD pattern of Fig. 5(a) with a zone axis [0 1 1]. Diffraction spots appear with respect to the $(1\,1\,\bar{1})$ plane, confirming the thin lamellae constitute a $\{1\,1\,1\}$ twin relationship. When the processing temperature was increased, deformation twins were also observed but only in some of grains. Fig. 5(d)–(f) show the microstructures of deformation twins in the samples processed at 700, 800 and 900 °C, respectively. It can be seen that there are only individual twin lamellae, but not twin bundles, in some grains. The lack of twin prevalence in these samples implies that twinning is not a dominant deformation mode at such high processing temperature, which is consistent with the optical observations as shown in Fig. 2(e)–(g).

In metallic materials with fcc structure, the formation of deformation twins is not only controlled by the characteristic of materials, such as SFE, but also by many deformation conditions, including strain, strain rate and temperature, etc. [31]. It is well accepted that high strain level, high strain rate and low temperature promote twin formation [31,32]. Decrease in SFE also facilitates deformation twinning because the cross-slip of dislocation becomes difficult. However, at elevated temperature, the SFE of materials could vary. Latanision and Ruff [33] had measured that the SFE of 304L SS increased from 16.4 mJ/m^2 at 25 °C to 27.6 mJ/m^2 at 135 °C and 30.4 mJ/m^2 at 325 °C. In the present case, the SFE of 304L SS could be increased up to relatively high level at 900 °C (for simplicity, 4 mJ/m^2 is increased every 100 °C based on the results of Latanision and Ruff [33], and then, the SFE of ~52 mJ/m^2 is roughly estimated at 900 °C). The increase of SFE suggests that deformation twinning becomes difficult due to the decrease of the resistant stress for dislocation slip that makes slip a very sufficient deformation mode. Therefore, deformation conditions required for twinning at high temperature should be more rigorous than those at low temperature. On one hand, the local stress resulted from stress concentration should be high up to the level of the critical twinning stress. In the case of the processing of austenitic SS (present 304L SS and previous 316L SS [17]), the high stress level can be achieved by dynamic strain aging, high strain level $(\varepsilon - 1)$ and relatively high strain rate (2 s^{-1}, 12.7 mm/s) during ECAP, as indicated by Yacipi et al. [17]. On the other hand, a favorable grain orientation is also necessary because only one twinning system, $\{1\,1\,1\}\langle 1\,1\,2\rangle$, can be activated in the fcc materials. For example, Huang et al. [34] had indicated recently that in order to twinning for Cu at RT and low stain rate under ECAP, the shear stress should be along the crystallographic direction of [1 1 2] and perpendicular to the direction of twin dislocation.

3.2. Tensile properties

Fig. 6(a) shows the typical tensile engineering stress–strain curves of the ECAPed samples. For comparison, the tensile curve of initial sample is also presented. It can be seen that the strength is substantially enhanced after ECAP deformation together with quite good elongation of all samples. Fig. 6(b) shows the dependence of yield strength (0.2% proof stress), ultimate tensile strength (UTS) and the value of elongation-to-failure on the processing temperature for the ECAPed 304L. At processing temperature of 500 °C, the yield strength can be increased from 165 MPa of initial state up to 810 MPa, and the UTS strength is increased from 550 to 895 MPa. However, there is an obvious decrease in the strength for the sample processed at 700 °C than that at 600 °C. With further increasing the processing temperature, the UTS strength varies little, while the yield strength decreases continuously. The elongation-to-failure of the ECAPed samples increases gradually with increasing the processing temperature. The best combination of both high yield strength and large elongation-to-failure takes place at 800 °C (605 MPa and 37%).

In most cases, the materials processed by SPD exhibited very high strength but generally low ductility due to the lack of strain hardening ability, regardless of cold and warm pressing [4,5,35–37]. In order to reveal the strain hardening behavior of the present samples, the engineering stress–strain curves in Fig. 6(a) were converted into the true stress–strain curves using

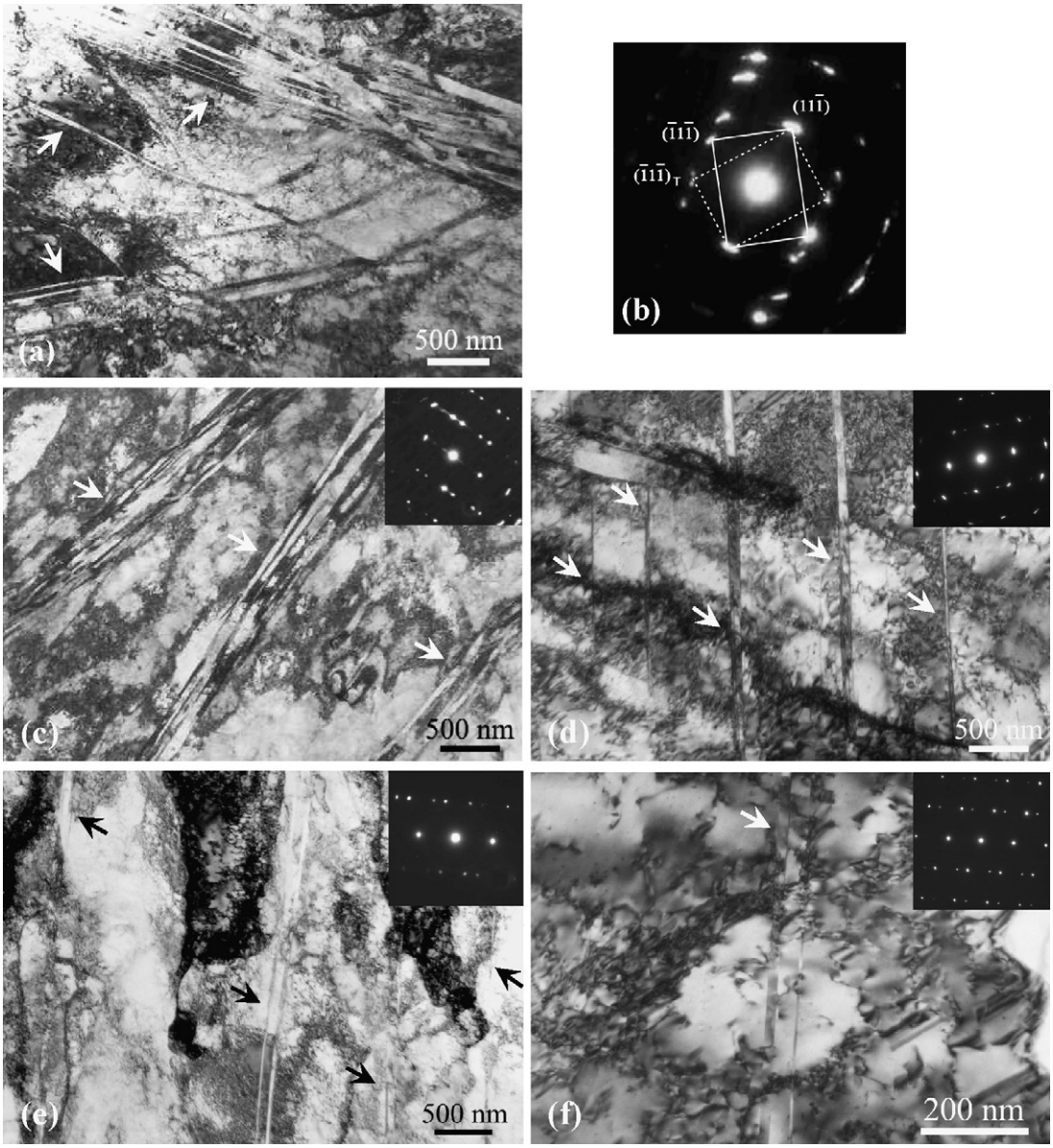

Fig. 5. Bright-field TEM micrographs with corresponding SAD patterns showing the microstructures of the samples processed at: (a) 500 °C, (b) corresponding SAD pattern of (a), (c) 600 °C, (d) 700 °C, (e) 800 °C, and (f) 900 °C, respectively. Deformation twins are indicated by arrows.

the following standard formulas:

$$S = (1 + \varepsilon) \cdot \sigma, \tag{1}$$

$$e = \ln(1 + \varepsilon), \tag{2}$$

where S is true stress, e the true strain, σ the engineering stress and ε is the engineering strain. The true stress–strain curves are shown in Fig. 6(c). Since the strain hardening exponent (n) for samples can be derived by fitting the Hollomon equation $\sigma = K\varepsilon^n$ to the uniform plastic deformation section of the true stress–strain curves well beyond the yield point, the calculated results are shown in Fig. 6(d). It is found that the n values follow a slow increasing order of 0.110, 0.147 and 0.175, respectively, for the samples processed at 500, 700 and 900 °C, but are much smaller than that (0.478) for the initial CG state. The decrease in n value should be owing to the microstructural refinement and high density of dislocations induced during the ECAP process, which hinder the subsequent dislocation storage during tensile deformation. However, the positive n value for the ECAPed samples indicates that certain strain hardening can occur prior to failure, which is especially prominent for the samples processed at temperature higher than 700 °C ($n > 0.15$).

The differences in strength evolution and strain hardening behavior can be explained by examining the microstructures of the samples processed at different temperatures. As shown in Fig. 3, the microstructures in the samples ECAPed at 500 and 600 °C are mainly characterized by lamellar structures and subgrains with small size, which are similar to those of cold-deformed fcc metals [10,36,37]. Therefore, a high strength but low ductility is expected. In contrast, the recovered microstructures, more equiaxed subgrains with a little large size and low dislocation density formed at higher pro-

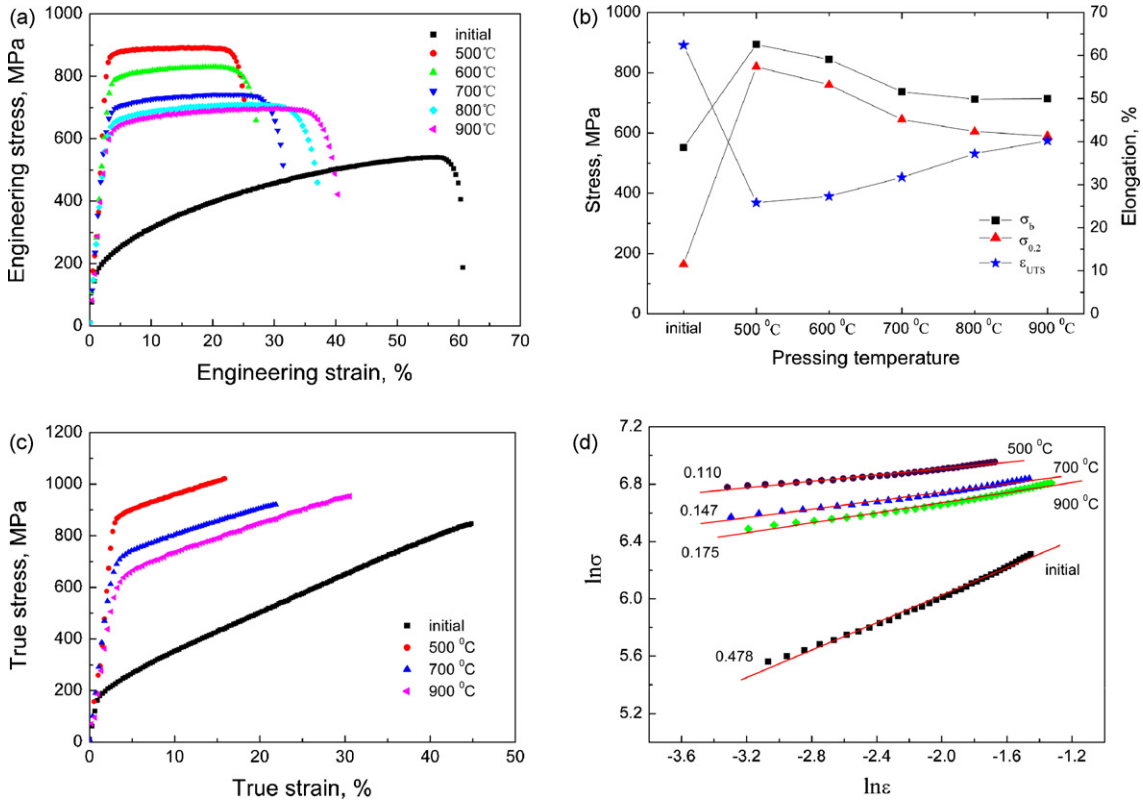

Fig. 6. Mechanical properties of 304L SS processed by ECAP: (a) engineering stress–strain curves, (b) the evolution of yield strength ($\sigma_{0.2}$), ultimate tensile strength (σ_b) and the value of elongation-to-failure (ε_{UTS}), (c) true stress–strain curves, (d) strain-hardening rate determined from the relationship between $\ln\sigma$ and $\ln\varepsilon$.

cessing temperature, can supply relatively low yield strength but high ductility. The increase of the processing temperature provides an effect similar to annealing as widely observed in pure ultrafine-grained Cu [38], Al alloys [13,15] and low-carbon steel [39], which obviously decreases the dislocation density and internal stress, and then lowers the strength but enlarges the ductility. On the other hand, the formation of deformation twins is also different with increasing the processing temperature. As is well known, the twin boundary is a strong obstacle to dislocation slip, which provides an effective strengthening similar to grain boundaries [40]. The more plenty of the twin boundaries are, the higher the strength is [41].

4. Conclusions

304L austenitic SS was successfully processed by ECAP in the temperature range of 500–900 °C. At temperature below 700 °C, the microstructures were characterized by lamellar structures and many bundles of deformation twins. These microstructures exhibited high tensile strength but low elongation-to-failure. With increasing the processing temperature, dynamic and also static recovery took place and more equiaxed subgrains with low dislocation density were obtained, together with a selected formation of individual twin band in some grains. The strain hardening ability of hot-processed ECAPed 304L SS is positive, but remarkably lower than that of initial state. The best combination of both high strength and large elongation-to-failure took place at the sample processed at 800 °C.

Acknowledgements

This research was financially supported by the National Natural Sciences Foundation of China (NSFC) under Grant nos. 50701047 and 50371090. The financial support by “Hundred of Talents Project” of Chinese Academy of Sciences and the National Outstanding Young Scientist Foundation for Zhang ZF under Grant no. 50625103 are also acknowledged.

References

[1] B.P. Kashyap, K. Tangri, Acta Metall. Mater. 43 (1995) 3971.
[2] O.V. Rybal’chenko, S.V. Dobatkin, L.M. Kaputkina, G.I. Raan, N.A. Krasilnikov, Mater. Sci. Eng. A387–A389 (2004) 244.
[3] R.Z. Valiev, R.K. Islamgaliev, I.V. Alexandrov, Prog. Mater. Sci. 45 (2000) 103.
[4] D.H. Shin, Y.S. Kim, E.J. Lavernia, Acta Mater. 49 (2001) 2387.
[5] Y. Fukuda, K. Oh-Ishi, Z. Horita, T.G. Langdon, Acta Mater. 50 (2002) 1359.
[6] Y.II. Son, Y.K. Lee, K.T. Park, C.S. Lee, D.H. Shin, Acta Mater. 53 (2005) 3125.
[7] J.T. Wang, X. Cheng, Z.D. Zhong, Z.Q. Guo, T.G. Langdon, Mater. Sci. Eng. A410–A411 (2005) 312.
[8] K.T. Park, Y.S. Kim, J.G. Lee, D.H. Shin, Mater. Sci. Eng. A293 (2000) 165.
[9] K. Nakashinma, Z. Horita, M. Nemoto, T.G. Langdon, Acta Mater. 46 (1998) 1589.

[10] Y. Iwahashi, Z. Horita, M. Nemoto, T.G. Langdon, Acta Mater. 46 (1998) 3317.
[11] M. Furukawa, Y. Iwahashi, Z. Horita, M. Nemoto, T.G. Langdon, Mater. Sci. Eng. A257 (1998) 328.
[12] P.B. Berbon, M. Furukawa, Z. Horita, M. Nemoto, T.G. Langdon, Metall. Mater. Trans. A30 (1999) 1989.
[13] A. Yamashita, D. Yamaguchi, Z. Horita, T.G. Langdon, Mater. Sci. Eng. A287 (2000) 100.
[14] Y.Y. Wang, P.L. Sun, P.W. Kao, C.P. Chang, Scripta Mater. 50 (2004) 613.
[15] Y.C. Chen, Y.Y. Huang, C.P. Chang, P.W. Kao, Acta Mater. 51 (2003) 2005.
[16] W.H. Huang, C.Y. Yu, P.W. Kao, C.P. Chang, Mater. Sci. Eng. A366 (2004) 221.
[17] G.G. Yapici, I. Karaman, Z.P. Luo, H.J. Maier, Y.I. Chumlyakov, J. Mater. Res. 19 (2004) 2268.
[18] B.Q. Han, E.J. Lavernia, F.A. Mohamed, Metall. Mater. Trans. 34A (2003) 71.
[19] I. Karaman, G.G. Yapici, Y.I. Chumlyakov, I.V. Kireeva, Mater. Sci. Eng. A410–A411 (2005) 243.
[20] I.P. Semenova, G.I. Raab, L.R. Saitova, R.Z. Valiev, Mater. Sci. Eng. A387–A389 (2004) 805.
[21] I. Karaman, A.V. Kulkarni, Z.P. Luo, Philos. Mag. 85 (2005) 1729.
[22] Q. Wei, K.T. Ramesh, E. Ma, L.J. Kesckes, R.J. Dowding, V.U. Kazykhanov, R.Z. Valiev, Appl. Phys. Lett. 86 (2005) 101907.
[23] A. Belyakov, T. Sakai, H. Miura, Mater. Trans. JIM 41 (2000) 476.
[24] A. Belyakov, K. Tsuzaki, H. Miura, T. Sakai, Acta Mater. 51 (2003) 847.
[25] S. Qu, C.X. Huang, Y.L. Gao, G. Yang, Q.S. Zang, Z.F. Zhang, Mater. Sci. Eng. A 475 (2008) 207–216.
[26] C.X. Huang, Y.L. Gao, G. Yang, S.D. Wu, G.Y. Li, S.X. Li, J. Mater. Res. 21 (2006) 1687.
[27] C.X. Huang, G. Yang, Y.L. Gao, S.D. Wu, S.X. Li, J. Mater. Res. 22 (2007) 724.
[28] V. Tsakiris, D.V. Edmonds, Mater. Sci. Eng. A273–A275 (1999) 430.
[29] A. Belyakov, W. Gao, H. Miura, T. Sakai, Metall. Mater. Trans. 29A (1998) 2957.
[30] A. Goloboroko, O. Sitdikov, T. Sakai, R. Kaibyshev, H. Miura, Mater. Trans. 44 (2003) 766.
[31] J.W. Christian, S. Mahajan, Prog. Mater. Sci. 39 (1995) 1.
[32] J.A. Venables, Philos. Mag. 63 (1961) 379.
[33] R.M. Latanision, A.W. Ruff Jr., Metall. Trans. 2 (1971) 505.
[34] C.X. Huang, K. Wang, S.D. Wu, Z.F. Zhang, G.Y. Li, S.X. Li, Acta Mater. 54 (2006) 655.
[35] D. Jia, Y.M. Wang, K.T. Ramesh, E. Ma, Y.T. Zhu, R.Z. Valiev, Appl. Phys. Lett. 79 (2001) 611.
[36] F. Dalla Torre, R. Lapovok, J. Sandlin, P.F. Thomson, C.H.J. Davies, E.V. Pereloma, Acta Mater. 52 (2004) 4819.
[37] D.R. Fang, Z.F. Zhang, S.D. Wu, C.X. Huang, H. Zhang, N.Q. Zhao, J.J. Li, Mater. Sci. Eng. A426 (2006) 305.
[38] Y.M. Wang, E. Ma, M.W. Chen, Appl. Phys. Lett. 80 (2002) 2395.
[39] D.H. Shin, J.J. Pak, Y.K. Kim, K.T. Park, Y.S. Kim, Mater. Sci. Eng. A325 (2002) 31.
[40] S. Asgari, E. El-Danaf, S.R. Kalidindi, R.D. Doherty, Metall. Mater. Trans. A28 (1997) 1781.
[41] Y.F. Shen, L. Lu, Q.H. Lu, Z.H. Jin, K. Lu, Scripta Mater. 52 (2005) 989.